PCCP

PERSPECTIVE

View Article Online
View Journal | View Issue

Cite this: *Phys. Chem. Chem. Phys.*, 2015, **17**, 10316

Temperature driven p–n–p type conduction switching materials: current trends and future directions

Satya N. Guin and Kanishka Biswas*

Received 29th December 2014,
Accepted 19th March 2015

DOI: 10.1039/c4cp06088a

www.rsc.org/pccp

Modern technological inventions have been going through a "renaissance" period. Development of new materials and understanding of fundamental structure–property correlations are the important steps to move further for advanced technologies. In modern technologies, inorganic semiconductors are the leading materials which are extensively used for different applications. In the current perspective, we present discussion on an important class of materials that show fascinating p–n–p type conduction switching, which can have potential applications in diodes or transistor devices that operate reversibly upon temperature or voltage change. We highlight the key concepts, present the current fundamental understanding and show the latest developments in the field of p–n–p type conduction switching. Finally, we point out the major challenges and opportunities in this field.

1. Introduction

Semiconductors are fundamental to modern electronics. In recent years, there has been growing interest in the development of novel inorganic semiconductors for application in transistors, switches, memory devices and sensors, which can be operated using an external stimulus.[1] The switching of material properties by applying external stimuli is interesting from both the fundamental point of view as well as for a number of advanced technologies.[1a,2] Important and interesting properties arise mostly during or within the phase transitions in solid state inorganic materials. Structural phase transformation is a common phenomenon in materials that are of fundamental interest to solid state inorganic chemistry.[3,4] Besides structural rearrangement, many of the solids undergo the orientation

New Chemistry Unit, Jawaharlal Nehru Centre for Advanced Scientific Research (JNCASR), Jakkur P.O., Bangalore 560 064, India. E-mail: kanishka@jncasr.ac.in

Satya N. Guin

Satya Narayan Guin received his BSc (2009) and MSc (2011) degree in chemistry from the University of Kalyani, Kalyani, West Bengal, India. He is currently pursuing his PhD at New Chemistry Unit, Jawaharlal Nehru Centre for Advanced Scientific Research (JNCASR), Bangalore, India. His research topics focus on thermoelectric energy conversion based on metal chalcogenides.

Kanishka Biswas

Kanishka Biswas obtained his PhD degree from Solid State and Structural Chemistry Unit, Indian Institute of Science, India (2009), and did his postdoctoral research at the Department of Chemistry, Northwestern University, USA (2009–2012). He is now an assistant professor (Faculty Fellow) in the New Chemistry Unit of Jawaharlal Nehru Centre for Advanced Scientific Research (JNCASR), Bangalore, India. He is the recipient of Ramanujan Fellowship from the Department of Science & Technology, India. He is a Young Associate of Indian Academy of Sciences, Bangalore. He is pursuing research in solid state chemistry, structure–property-correlations of metal chalcogenides, thermoelectrics and topological insulators.

change of the electron clouds influencing the state of electron spin during phase transition. Such changes in the crystal structures, electron clouds and electron spin states can give rise to changes in the electronic structure and phonon dispersion of the inorganic materials. During phase transition, widening or narrowing the band gap of the material can result in insulator or metallic states, respectively, in the same material, which controls the carrier concentration and electronic properties.[5,6] Collectively, structural rearrangements, changes in electronic or spin structures and phonon dispersions lead to novel physical properties, such as superconductivity,[7] superionic conduction,[5,8–13] optical storage,[14a] the photoelectronic effect,[14b–e] the giant magnetocaloric effect,[15] giant magnetoresistance,[16] p–n–p or p–n type conduction switching[2,6,16,17] and thermoelectricity.[8,9,18–22] Design and control of the changes in physical properties associated with a phase transition have been key to the development of current functional materials.[17] Among the various important physical properties, temperature dependent p–n–p type conduction switching is a relatively new phenomenon, which can have fascinating applications in modern electronics such as in diodes or transistor devices that operate reversibly upon temperature or voltage change near room temperature.

Although there is no general protocol or theory that can predict the conduction type switching of a single material, the existence of a semimetallic intermediate state in the electronic structure during phase transition is known to be responsible for p–n–p type conduction switching in several inorganic materials.[2,6,16,17]

The primary requirement for p–n–p type conduction switching is the suitable change in electronic structure, which can be triggered either by the change in temperature or electric voltage. Secondly, the thermal conductivity of the material should be low enough for maintaining the appropriate temperature gradients for separation of different carrier type regions in a single compound. Finally, temperature of the p–n–p type conduction switching must be closer to the room temperature, so that the device can be used for practical purposes with a temperature gradient near ambient temperature. To date only a few compounds have been discovered that show such fascinating p–n–p type conduction switching properties. The field of conduction type switching presents an important challenge to synthetic chemists, physical chemists, physicists as well as material scientists. The discovery of new promising materials requires a combination of theoretical guidance, keen chemical intuition, synthetic chemistry expertise, materials processing, and good measurement skills. In this perspective, we cover the key concepts in the field of p–n–p type conduction switching, present the current understanding, and show the latest developments.

2. State-of-the-art materials

State-of-the-art materials that show the temperature dependent p–n–p type conduction switching are mostly noble metal based binary, ternary or quaternary chalcogenides and chalcogenide halides. This class of compounds generally show Ag^+/Cu^+ ion conduction in their superionic phase, while the chalcogen or chalco-halogen sublattice are found to be static. Fig. 1 shows the p–n–p type conduction switching in the state of art inorganic compounds such as $Ag_{10}Te_4Br_3$, $AgBiSe_2$, AgCuS, and $Ag_{10}Te_4Br_{2.6}Cl_{0.4}$.[2,6,17,23] Temperature dependent Seebeck coefficient (S) analysis is the direct measurement for the temperature dependent conduction type change, because the sign of S denotes the carrier type of a particular material. The positive sign of the S indicates p-type conduction, whereas the negative sign denotes n-type conduction. The change in the magnitude of Seebeck during p–n–p type conduction switching in $Ag_{10}Te_4Br_3$, $AgBiSe_2$, AgCuS, and $Ag_{10}Te_4Br_{2.6}Cl_{0.4}$ are 1400, 730, 1760 and 1800 $\mu V\ K^{-1}$, respectively.[2,6,17,23] Temperatures of the p–n–p type transition in several compounds are given in Table 1.

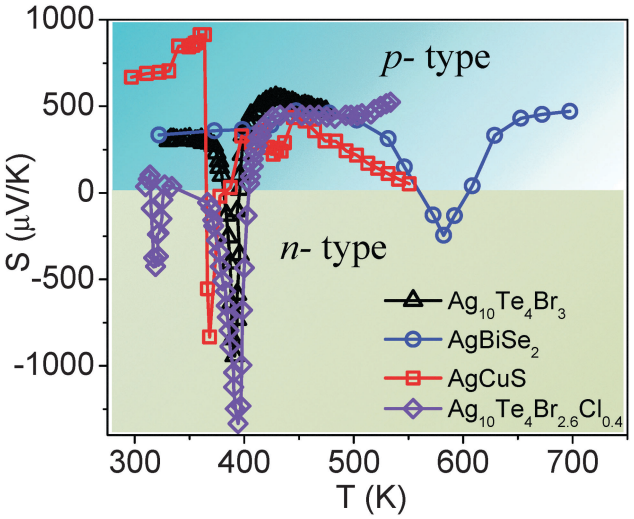

Fig. 1 Current state of the art materials which show p–n–p conduction switching as a function of temperature. Seebeck coefficient (S) *vs.* temperature data of important chalcogenides and chalcogenide-halides.

Table 1 p–n–p transition temperatures of the state of art materials

Material	Transition temperature (K)
$Ag_{10}Te_4Br_3$ (ref. 2)	380
$AgBiSe_2$ (ref. 6)	560
AgCuS (ref. 17)	360
$Ag_{10}Te_4Br_{2.6}Cl_{0.4}$ (ref. 23)	400

3. Noble metal chalcogenide halides

Noble metal polychalcogenide halides represent a new class of materials which show an intriguing phase behaviour, structural variability, a high degree of disorder and high ion dynamics.[2,24] These compounds are based on substructures of isolated cations and anions; and they exhibit mixed ionic and electronic conduction due to the changes in the substructure of the mobile ion with the function of temperature.[2,25,26] Ternary silver chalcogenide halide has been investigated for more than 40 years.[27] Interestingly, silver forms the highest number of known ternary phases compared to that of the copper and gold

chalcogenide halide analogues.[27] In the last few years, diverse classes compounds of coinage metal chalcogenide halides and polychalcogenide halides have been discovered, such as: Ag_5Q_2X with Q = S/Se/Te and X = Cl, Br,[28–36] Ag_3SX,[37] $Ag_{19}Q_6X_7$,[38] $Ag_{10}Q_4X_3$ with Q = S/Se/Te and X = Cl/Br/I,[27,39,40] $Ag_{23}Te_{12}X$ with X = Cl/Br[41] and $Ag_{20}Te_{10}X_2$ with X = Br/I.[24] Some of these compounds belong to either the quasibinary phase between AgX–Ag_2Q (*e.g.* Ag_3QX, Ag_5Q_2X, Ag_6TeBr_4) or solid solutions or even to a new class of materials.[25,27,42] Most of these compounds have been characterized by their ion mobility and polymorphism.[42] Tom Nilges and co-workers have extensively explored several new compounds in the silver(I) ploychalcogenide halide family and investigated their electronic and thermoelectric properties. Structures of these compounds are generally complex and crystal structure refinement becomes difficult due to the dynamic disorder within the cation and anion substructures.[42] Detailed structural description and discussion on the thermoelectric properties are beyond the scope of the present perspective. Here, we have only focused on the conduction type switching property of these compounds.

$Ag_{10}Te_4Br_3$ is the first discovered compound of this class, which shows p–n–p type conduction switching.[2] Existence of four polymorphs were reported for $Ag_{10}Te_4Br_3$.[2,25,39,40] Two reversible phase transitions were observed near room temperatures. δ-$Ag_{10}Te_4Br_3$ transforms to γ-$Ag_{10}Te_4Br_3$ at 290 K, whereas γ-$Ag_{10}Te_4Br_3$ transforms to β-$Ag_{10}Te_4Br_3$ at 317 K.[2] A third structural phase transition (β–α) was observed at ~390 K.[2] Although little change in volume was observed during all the structural transitions, a substantial change in the dimensionality of the Ag ion distribution, from an exclusively 2-dimensional (δ and γ) to a 3-dimensional (β and α) arrangement, was observed with increasing temperature.[39] The enhanced Ag ion dynamics and mobility in the covalently bonded tellurium substructure at elevated temperature resulted in structural frustration and disorder phenomena in β and α polymorphs. A detailed structural description of the different polymorphs related to the phase transition can be found elsewhere.[39] The electronic conductivity is generally superior to that of the ionic conductivity by typically one order of magnitude in the case of all the polymorphs of $Ag_{10}Te_4Br_3$.[2]

Temperature dependent Seebeck measurement shows a clear p–n–p type conduction switching in $Ag_{10}Te_4Br_3$ (Fig. 2).[2] During broad (β–α) phase transition (see DSC curve in Fig. 2), the Seebeck coefficient changes signs from 310 μV K^{-1} in the β-phase to −940 μV K^{-1}. With further increasing temperature, the Seebeck coefficient again changes its sign resulting in a value of 540 μV K^{-1} in α-$Ag_{10}Te_4Br_3$ with a drop in Seebeck (ΔS) of ~1400 μV K^{-1}.[2] This process was further confirmed by a temperature dependent potentiometric study and steady state polarization measurement, which indicated a substantial drop in chemical potential for Ag ions upon going from the γ to β to α phase with increasing temperature.[2] However, chemical potential of the anions was increased in the opposite direction towards higher values. Structural changes in the Te sublattice were believed to be responsible for the switching of chemical potentials of the components.

In the γ-$Ag_{10}Te_4Br_3$ phase, the Te_4 subunit is coordinated by silver, which forms a linear strand $[AgTe_4]_n$ along the crystallographic *c* axis.[2] The disordering of Ag^+ ions initiates during the γ–β phase transition at 317 K, within the $[AgTe_4]_n$ strands. However, the Ag^+ ion starts to leave out from the $[AgTe_4]_n$ strand at about 390 K during β–α transition (Fig. 3).[2] Reorganisation of

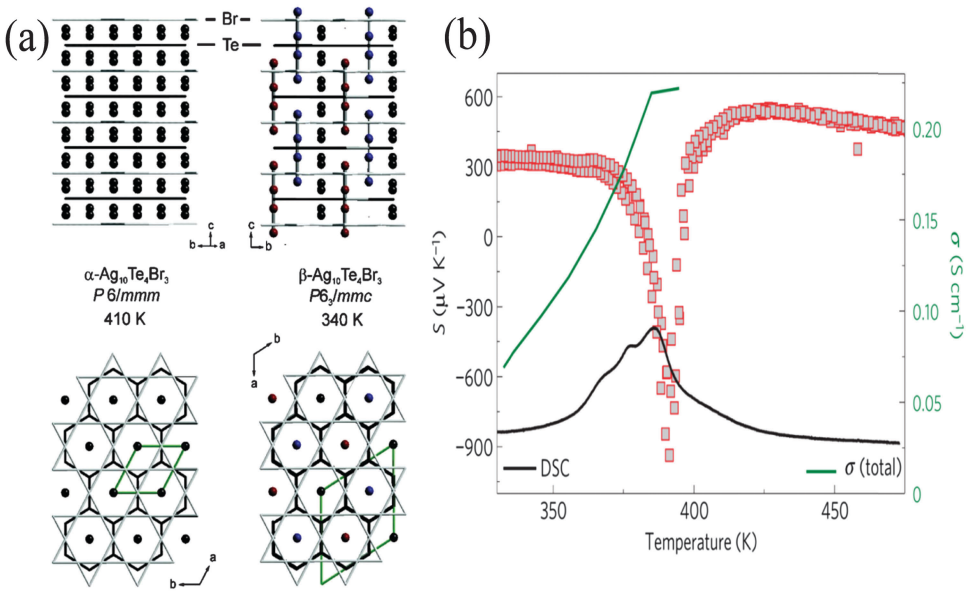

Fig. 2 (a) Structure sections of different phases of $Ag_{10}Te_4Br_3$. Anion substructure: Te^{2-} (dark gray) and Br^- (light gray) ions are connected by solid lines. (b) Temperature dependent electrical conductivity (*σ*), Seebeck coefficient (*S*) and DSC data for $Ag_{10}Te_4Br_3$. A pronounced peak in the Seebeck coefficient with two changes in the sign of the value was observed for $Ag_{10}Te_4Br_3$. Panels (a) and (b) were adapted with permission from ref. 39 (*Chem. Mater.* 2007, **19**, 1401–1410) © 2007 American Chemical Society and ref. 2 (*Nat. Mater.*, 2009, **8**, 101–108) © 2009 Nature Publishing Group, respectively.

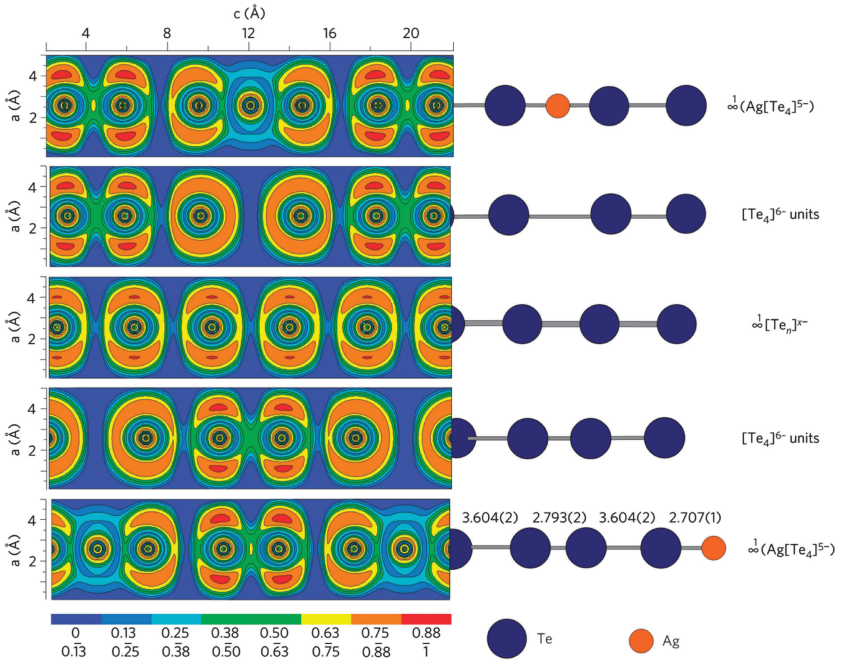

Fig. 3 Electron localization function (ELF) analysis of the polyanionic substructure of $Ag_{10}Te_4Br_3$. The dynamic process of the abstraction of the silver ions results in the formation of an equidistant Te chain within the anion substructure of $Ag_{10}Te_4Br_3$. A relaxation of the polyanionic $[Te_4]^{6-}$ unit takes place during the abstraction process. Adapted with permission from ref. 2 (*Nat. Mater.*, 2009, **8**, 101–108) © 2009 Nature Publishing Group.

the Te_4 entity resulted in a reshuffle of the electronic bands with an intermediate quasi-metallic state.[2] The change in the conduction type from p to n-type resulted due to the upwards shift of the Fermi level in the band, which was triggered due to generation of extra conduction electrons in higher band states. The change in electron concentration occurred due to the electronic change in the tellurium substructure. The linear strand (Te^{2-}) acted as a reservoir of electrons that were set free by the formation of oligomeric units (Te_4^{6-}). The redox step involved in the formation of continuous chain Te^{2-} by breaking Te_2^{2-} dumbbell bonds with consumption of electrons during β–α phase transition made the material p-type at high temperatures (Fig. 4).[1a,2]

Substitution within the cation and anion substructures has a tremendous effect on physical properties and can effectively tune phase transition temperature.[43,44] In order to shift the temperature driven p–n–p type conduction switching to an applicable temperature, various cationic/anioinic substitutions in $Ag_{10}Te_4Br_3$ were investigated.[23] Although little shift in transition temperature was observed with 2 mol% iodine doping ($Ag_{10}Te_4Br_{2.8}I_{0.2}$), but the jump in the Seebeck coefficient was much smaller compared to that of pristine $Ag_{10}Te_4Br_3$ (Fig. 5).[23] Interestingly, the solid solution $Ag_{10}Te_4Br_{2.6}Cl_{0.4}$ shows a significant jump in the Seebeck coefficients with a $\Delta S \sim 1800\ \mu V\ K^{-1}$ (Fig. 1 and 5).[23] Sulphur and selenium substitution on the Te sublattice resulted in the complete disappearance of the p–n–p conduction switching (Fig. 5),[23] because the Peierls distortion within the covalently bonded Te-substructure was disturbed effectively by a lightered homologue, sulphur or selenium.[23] Recently the partial substitution of copper ions on the cation sublattice of $Ag_{10}Te_4Br_3$ has been studied, which showed a clear change in the phase transition temperature in $Ag_{10}Te_4Br_3$.[45]

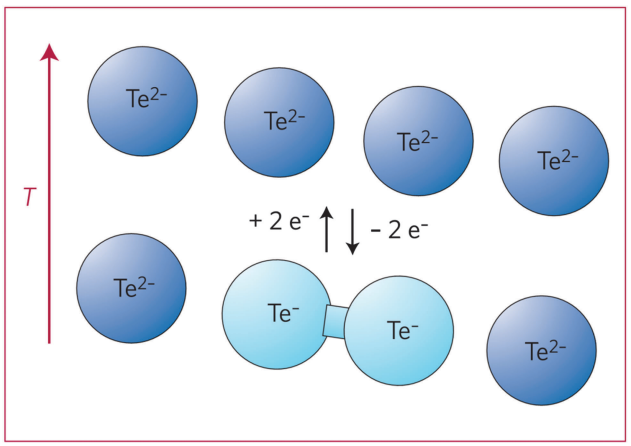

Fig. 4 Reversible redox switching in a poly-telluride chain. With increasing temperature, the Te_2^{2-} dumbbell pairs in the tellurium strands break up into two Te^{2-} ions. Adapted with permission from ref. 1*a* (*Nat. Mater.*, 2009, **8**, 88–89) © 2009 Nature Publishing Group.

4. Superionic noble metal chalcogenides

Superionic conductors are exciting materials that show unique solid liquid hybrid behaviour.[12] They allow the macroscopic movement of ions through their structure, leading to exceptionally high values (liquid-like) of ionic conductivity in the

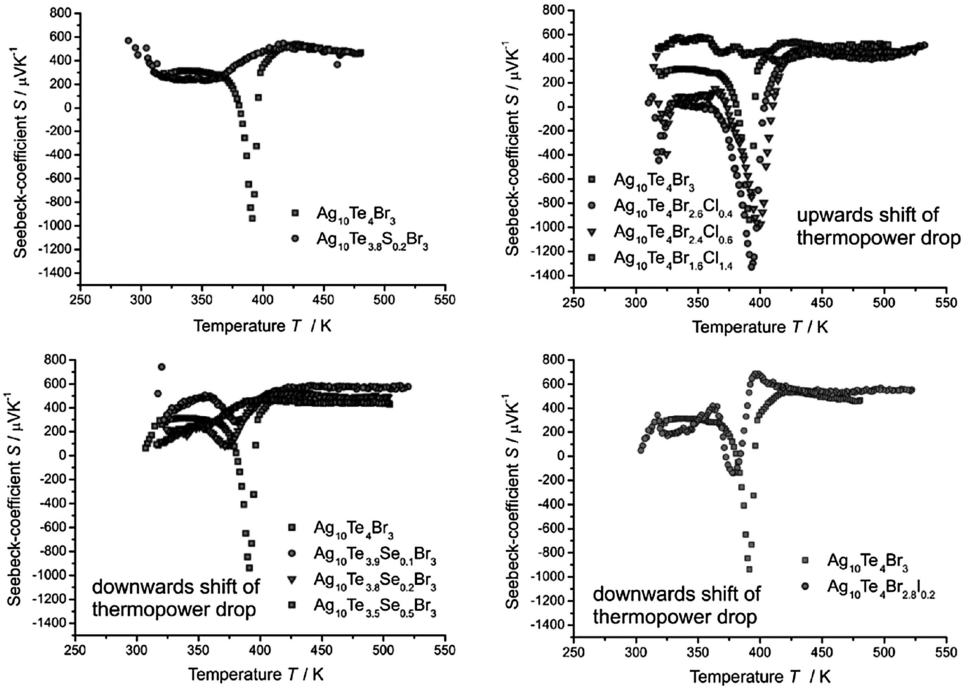

Fig. 5 Temperature dependent Seebeck-coefficients of the solid solution $Ag_{10}Te_{4-x}Q_xBr_{3-y}X_y$ with Q = S, Se and X = Br, I. Adapted with permission from ref. 23 (*Solid State Sci.*, 2011, **13**, 944–947) © 2011 Elsevier.

solid state.[10,12] The superionic transition normally happens above a critical temperature (mostly at elevated temperature). These materials are generally made of weakly coupled cationic and anionic substructures in which one type constituent species form a rigid framework, whereas another type constituent species occupies interstices.[10,17] At elevated temperature *i.e.* above superionic transition temperature, the rigid framework expands and frequently acquires a new symmetry, and allows the rapid diffusion of a significant fraction of the other constituent species within the rigid framework.[12,46] Superionic materials have been classified into three different types depending on how the superionicity arises: (a) Type I: superionicity arises due to a first-order structural phase transition, (b) Type II: High ionic conductivity arises due to a gradual and continuous disordering process within the same phase, (c) Type III: superionicity arises not due to clear phase transition, but *via* increased mobility of a number of thermally activated defects.[10]

In most of the cases, cations such as Ag^+, Cu^+, Li^+, H^+ show liquid-like behaviour in the respective superionic compounds. However in some cases, it has been reported that highly polarizable anions, like F^{2-}, O^{2-} can also exhibit superionic conduction.[10] A superionic label may be applied to a material whose ionic conduction is above $\sigma \sim 10^{-2}\ \Omega^{-1}\ cm^{-1}$, with the best superionic conductor achieving ionic conductivities as high as of $\sigma \sim 1\ \Omega^{-1}\ cm^{-1}$.[10,12] This high ionic conductivity makes these materials potential candidates for a number of technological applications.[2,17]

AgCuS is the only known compound to date of this class that shows p–n–p type conduction switching properties.[17] The existence of four different polymorphs as a function of temperature for AgCuS has been reported in the literature.[17,47–49] At room temperature, AgCuS is a p-type semiconductor and crystallizes in the ordered orthorhombic (β-AgCuS) phase. Below 120 K, AgCuS crystallizes in $Pmc2_1$ space group, which is a slightly distorted form of the room-temperature polymorph. These two low temperature polymorphs of AgCuS have ordered structure. As the temperature increases, β-AgCuS undergoes two superionic structural phase transitions, first to a partially disordered superionic hexagonal (α-AgCuS) phase at 361 K, and then to a fully disordered superionic cubic (δ-AgCuS) phase at 439 K (Fig. 6a).[47–49] Phase transitions in AgCuS are reversible in nature, which has been confirmed by synchrotron powder X-ray diffraction (Fig. 6b) and temperature dependent Raman spectroscopy measurement (Fig. 6c). Recently, we have found that AgCuS exhibits a fascinating reversible p–n–p type conduction switching along with a colossal jump in the thermopower (ΔS of $\sim$ 1757 μV K^{-1}) at $T \sim 364$ K during (β–α) superionic phase transition (Fig. 7a). More importantly, this property of AgCuS is more readily usable in a device, as the temperature of its transition ($T \sim 360$) is closer to room temperature compared to that of $AgBiSe_2$ ($T \sim 560$) and $Ag_{10}Te_4Br_3$ ($T \sim 380$ K). Temperature dependent electrical conductivity (σ) exhibited a sharp increase during (β–α) transition ($\sim$364 K), while the increase in σ during (α–δ) transition ($\sim$430 K) was not very significant (Fig. 7b). Furthermore, AgCuS also showed low thermal conductivity ($\sim$0.5 W mK^{-1}) over the 300–550 K temperature range (Fig. 7c), which enabled it to maintain required temperature gradients to form a p–n–p device based on a single compound. Temperature dependent Raman spectroscopy, positron annihilation spectroscopy measurements,

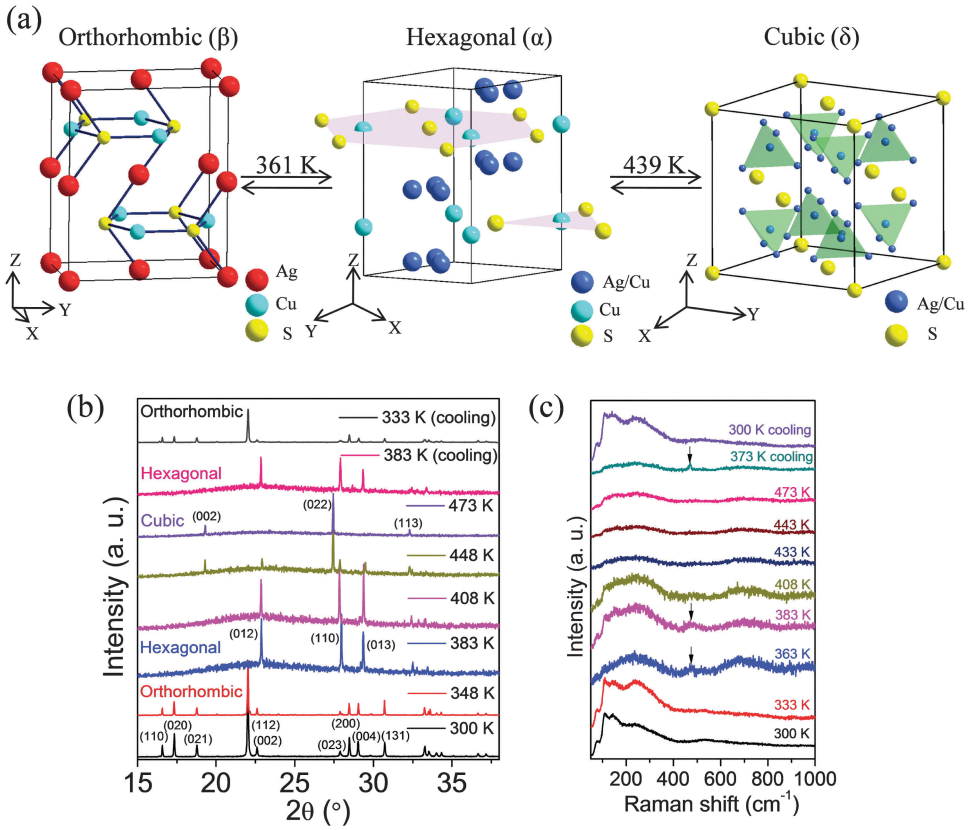

Fig. 6 (a) Structural evaluation of AgCuS as a function of temperature. Temperature dependent (300–473 K) heating–cooling cycle synchrotron (E = 12.42 keV and λ = 0.998 Å) powder X-ray diffraction patterns (b) and Raman spectra (c) of AgCuS. Black arrow in (c) indicates the characteristic Raman peak for Cu–S vibration. Adapted with permission from ref. 17 (*J. Am. Chem. Soc.*, 2014, **136**, 12712–12720) © 2014 American Chemical Society.

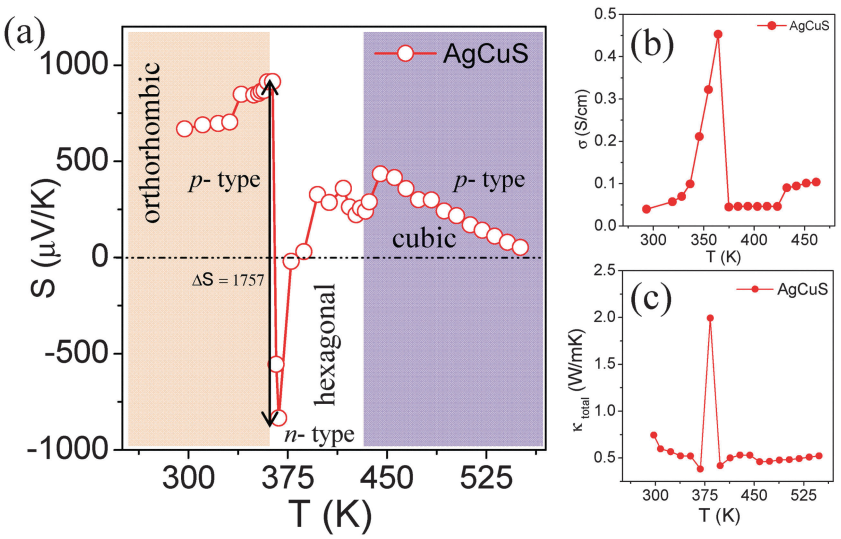

Fig. 7 Temperature dependent (a) Seebeck coefficient (S), (b) electrical conductivity (σ) and (c) total thermal conductivity (κ_{total}) of AgCuS. Adapted with permission from ref. 17 (*J. Am. Chem. Soc.*, 2014, **136**, 12712–12720) © 2014 American Chemical Society.

heat capacity and the electronic structure and phonon dispersion calculations were performed to understand the mechanism of p–n–p type conduction switching in AgCuS.[17]

Existence of semimetallic electronic states during (β–α) phase transition has been confirmed by density functional electronic structure calculations.[17] Due to atomic movement

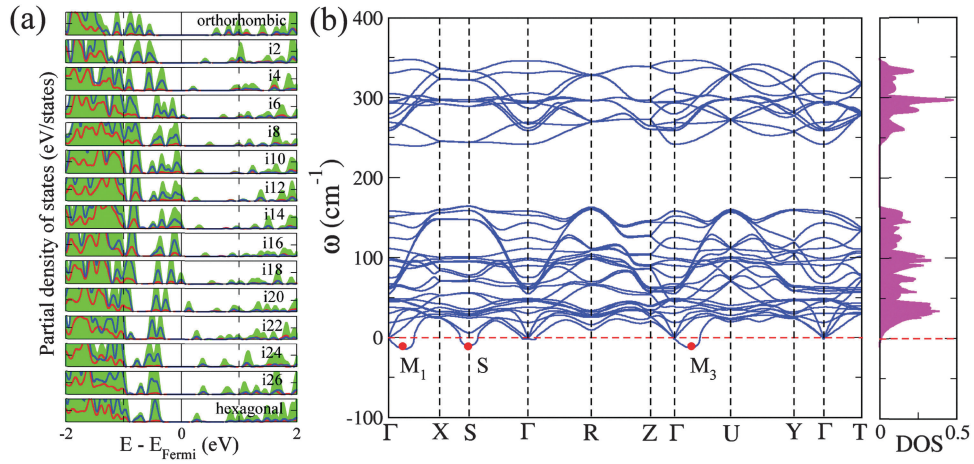

Fig. 8 (a) Partial density of states of AgCuS along the minimum energy path of orthorhombic to hexagonal phase transformation. Green, red and blue colours in (a) have been used to represent partial density of states of S-3p, Ag-4d and Cu-3d respectively. (b) Phonon dispersion plot and phonon density of state of β-AgCuS. Adapted with permission from ref. 17 (*J. Am. Chem. Soc.*, 2014, **136**, 12712–12720) © 2014 American Chemical Society.

involved in disordering of the cationic sublattice, there were changes in bonding reflected in mixing between the states in valence and conduction bands. This resulted in downward and upward shifts in the conduction and valence bands respectively. Overlapping of valence and conduction bands in a small energy interval near the gap resulted in an intermediate semimetallic state (Fig. 8a).[17] Existence of this semi-metallic states during the (β–α) transition was responsible for sharp increase in the temperature dependent electrical conductivity at 364 K (Fig. 7b). Ag vacancy was responsible for p-type conduction in β-AgCuS at room temperature and acted as an effective path for the movement of Ag atoms during (β–α) phase transition, whereas Cu–S bonds remained intact, which was confirmed by temperature dependent Raman spectroscopy (Fig. 6c). An intermediate semimetallic state, constituting of hybridized Cu–S orbitals, aroused from reshuffling of electronic orbitals contributing to valence and conduction bands during the orthorhombic to hexagonal phase transition (Fig. 8a), which was responsible for the p–n–p conduction switching in AgCuS.[17] Phonon dispersion of the orthorhombic β-AgCuS phase exhibited a gap that separates high energy modes originating from sulphur sublattice and low energy modes largely involving the Ag/Cu sublattices (Fig. 8b). These low frequency phonon modes were expected to soften further at higher temperature, and lead to flow of cations or liquid-like behaviour. Such liquid-like behaviour of the heavy cation sublattice resulted in effective phonon scattering, thereby reducing thermal conductivity in AgCuS. A rigid sulphur sublattice was primarily responsible for the electronic charge transport, whereas soft vibrations and mobility of Ag/Cu ions were responsible for the ultra-low thermal conductivity. Such decoupling of electronic and phonon transport resulted in a unique combination of temperature dependent p–n–p conduction switching and ultra-low thermal conductivity in AgCuS near room temperature.[17] Mention must be made that n–p type conduction switching has been observed in AgCuSe, where existence of an intermediate semi metallic state is also responsible for the switching in the conduction type.[50,51]

5. Disordered noble metal chalcogenides

I–V–VI_2 (where I = Cu, Ag, Au or alkali metal; V = As, Sb, Bi; and VI = S, Se, Te) type of compounds are a special class of semiconductors which are renowned for their intrinsically low thermal conductivity due to the strong anharmonicity of their bonding arrangements.[22,52,53] Some of the members of this class crystallize in cation disordered high symmetry cubic rock salt structure at room temperature (*e.g.* $AgSbSe_2$, $AgSbTe_2$, $NaBiTe_2$, $NaBiSe_2$, $NaSbSe_2$, $NaSbTe_2$ *etc.*).[53,54] However, few of the members show structural phase transitions as a function of temperature ($AgBiS_2$, $AgBiSe_2$, $AgBiTe_2$, *etc.*)[54] and finally transform to cation disordered rock salt cubic structure at high temperatures. The presence of a stereochemically active ns^2 lone pair on group V (Sb/Bi) element and disorder cation sublattice results in strong anharmonicity in bonding arrangements which gives rise to low thermal conductivity.[53] Recently the solid state chemistry community has taken a great interest in studying the thermoelectric property of these compounds due to their favourable electronic structure and glass like thermal conductivity.[6,19,21,22,55]

Recently, nanocrystals of $AgBiSe_2$ exhibited p–n–p type conduction switching during order–disorder phase transition.[6] $AgBiSe_2$ showed two structural phase transitions at higher temperatures.[54] Hexagonal to rhombohedral phase transition occurred at 460 K and with further increasing the temperature to 580 K ordered rhombohedral $AgBiSe_2$ transformed to a disordered cubic phase (Fig. 9a).[21] Interestingly p–n–p conduction switching was only observed when $AgBiSe_2$ was synthesized in its nanocrystalline form. The intrinsic conduction type at room temperature for bulk $AgBiSe_2$ is n-type, which is different from the nanocrystalline $AgBiSe_2$ (p-type). The positive sign of the Seebeck coefficient at room temperature indicated p-type conduction in the hexagonal phase of nanocrystalline $AgBiSe_2$.[5,6] During hexagonal–rhombohedral transition, the Seebeck coefficient increased from 390 $\mu V K^{-1}$ to 460 $\mu V K^{-1}$ at ~423 K; then it

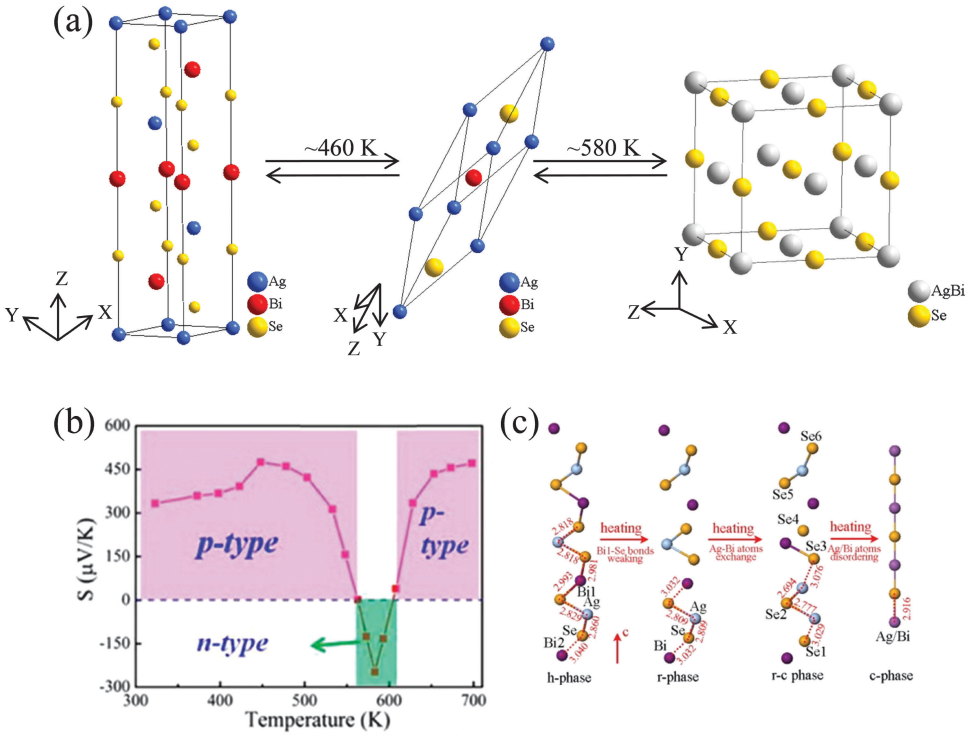

Fig. 9 (a) Crystal structural evolution among hexagonal, rhombohedral, and cubic phases of $AgBiSe_2$. (b) Temperature dependent Seebeck coefficient (*S*). (c) Schematic representations of the atomic rearrangement for the Ag–Bi–Se chain during the phase transition. Panels a and b, c were adapted with permission from ref. 21 (*J. Mater. Chem. A*, 2015, **3**, 648–655) © 2015 Royal Society of Chemistry and ref. 6 (*J. Am. Chem. Soc.* 2012, **134**, 18460–18466) © 2012 American Chemical Society respectively.

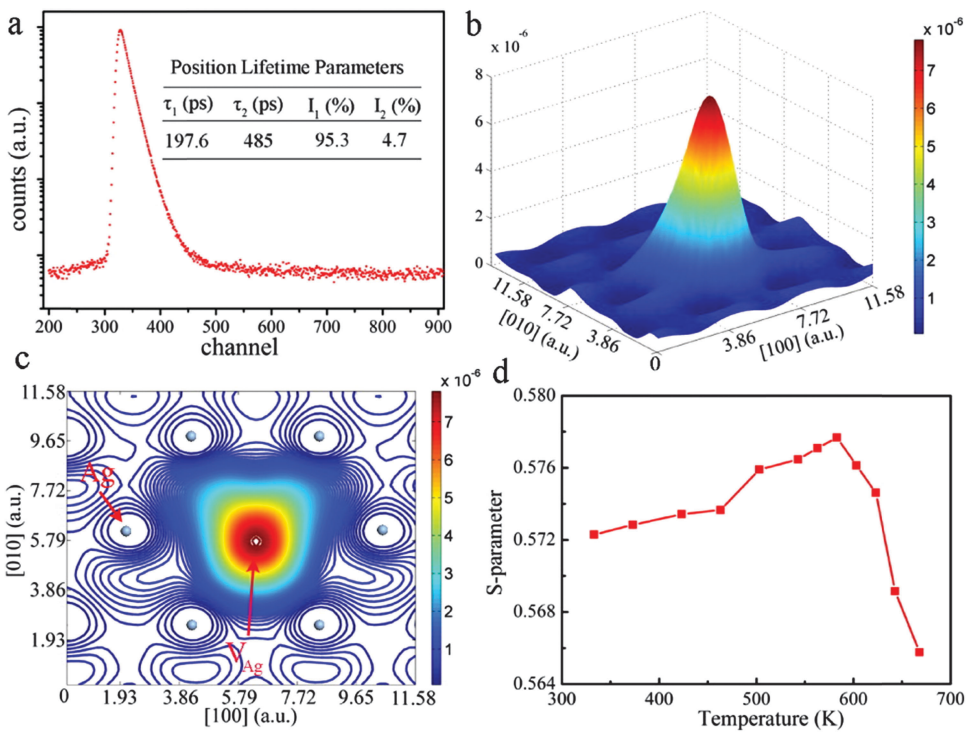

Fig. 10 (a) Positron lifetime spectrum of $AgBiSe_2$ nanocrystals yield two lifetime components, which are designed to the Ag vacancies and larger size defects respectively. (b and c) Schematic representations of trapped positrons for $AgBiSe_2$ nanocrystals in the basal plane and (001) plane. It is clearly seen that the positron is mostly trapped by negatively charged V_{Ag} (V_{Ag} denote Ag vacancy) in $AgBiSe_2$ nanocrystals. (d) Doppler broadening S parameter for $AgBiSe_2$ nanocrystals as a function of temperature. The S parameter approaches a maximum value at around 580 K indicating the most abundant valence electrons. Adapted with permission from ref. 6 (*J. Am. Chem. Soc.*, 2012, **134**, 18460–18466) © 2012 American Chemical Society.

underwent a broad order–disordered transition (~560 K) with a reversible p–n–p type conduction switching (Fig. 9b).[6] The Seebeck coefficient value has been changed from 480 μV K^{-1} to −250 μV K^{-1} and then reverted back to 470 μV K^{-1} during rhombohedral to cubic phase transition (Fig. 9b).[6] The Positron annihilation spectroscopy study of the $AgBiSe_2$ nanocrystal indicated that formation of Ag vacancies during solution phase synthesis, which was indeed responsible for p-type conduction in hexagonal and rhomboheral $AgBiSe_2$ phases (Fig. 10). Ag vacancy acted as a bridge of atoms during Ag/Bi bimetal exchange at the order–disorder phase transition (Fig. 9c).[6] This mechanism was further confirmed by temperature dependent Raman spectroscopy.[6] Electronic structure calculation revealed that Ag–Bi atoms exchange during rhombohedral–cubic transition brought changes in the density of states at the Fermi level, that resulted in an intermediate quasi-metallic state bringing more conduction electrons, which led to p–n–p type conduction swtiching.[6] During rhombohedral to cubic phase transition, Doppler broadening of the S parameter increased and reached maximum at around 580 K, indicating that the conduction in the system was mainly due to electrons (Fig. 10).[6] Nanoscrystalline $AgBiSe_2$ exhibited ultra-low thermal conductivity, especially in the cubic form. The disordered cation sublattice and bond anharmonicity softened the phonon at high temperature and resulted in low thermal conductivity. p–n–p conduction switching in $AgBiSe_2$ was observed only in the nanocrystalline form but not in narrow band gap bulk crystals.[19,21] It would be worth to search for p–n–p conduction switching in nanocrystals of known bulk chalcogenides with narrow band gaps. Recently, our group has studied thermoelectric properties of kinetically stable nanocrystalline cubic $AgBiS_2$.[20] Although the nanocrystalline $AgBiS_2$ compound has not exhibited any conduction switching, it has shown a sharp jump in the Seebeck coefficient at ~600 K, which has not been observed in the bulk form of $AgBiS_2$. The heat capacity measurement indicated that this observation was due to ordered–disordered transition in the nanocrystalline $AgBiS_2$.[20]

6. Conclusions and future outlook

In this perspective, we have discussed the recent advancements in the p–n–p type conduction switching materials which include fundamental structure–property correlations, understanding of the mechanisms and latest developments in this field. Currently discovered materials which show p–n–p type conduction switching property are mainly based on Ag/Cu based chalcogenides and chalcogenide halides. Generally, p–n–p type conduction switching occurred during order–disorder structural phase transition. The existence of an intermediate semimetallic electronic state during phase transition is known to play an important role in p–n–p type conduction switching in recently discovered inorganic materials. Till date the number of materials which show this unique property are very few. Design, synthesis, discovery of new materials and deeper understanding of structure–property are required to proceed further in this field. Better theoretical understanding is necessary, which can provide deeper insight into the electronic structure and phonon dispersion, and thus can offer important hints to tune the material property by band structure engineering. Furthermore, p–n–p transition temperature should be close to room temperature, so that the materials can be used in modern electronics and switches. These are truly possible upon collaborations among chemists, physicists, materials scientists and theoreticians. We expect that progress in this field will be continued and hope to see them as new/better candidates for future technological applications.

Acknowledgements

The authors thank New Chemistry Unit and Sheikh Saqr Laboratory, JNCASR, for financial support. K.B. acknowledges SERB, Govt. of India, for the Ramanujan Fellowship.

References

1 (*a*) J. Janek, *Nat. Mater.*, 2009, **8**, 88–89; (*b*) K. Terabe, T. Hasegawa, T. Nakayama and M. Aono, *Nature*, 2005, **433**, 47–50; (*c*) R. Waser and M. Aono, *Nat. Mater.*, 2007, **6**, 833–840.
2 T. Nilges, S. Lange, M. Bawohl, J.-M. Deckwart, M. Janssen, H.-D. Wiemhöfer, R. Decourt, B. Chevalier, J. Vannahme, H. Eckert and R. Weihrich, *Nat. Mater.*, 2009, **8**, 101–108.
3 C. N. R. Rao, *Acc. Chem. Res.*, 1984, **17**, 83–89.
4 C. N. R. Rao and J. Gopalakrishnan, *New directions in solid state chemistry*, Cambridge University Press, 2nd edn, 1997.
5 C. Xiao, J. Xu, K. Li, J. Feng, J. Yang and Y. Xie, *J. Am. Chem. Soc.*, 2012, **134**, 4287–4293.
6 C. Xiao, X. Qin, J. Zhang, R. An, J. Xu, K. Li, B. Cao, J. Yang, B. Ye and Y. Xie, *J. Am. Chem. Soc.*, 2012, **134**, 18460–18466.
7 E. Coronado, C. Marti-Gastaldo, E. Navarro-Moratalla, A. Ribera, S. J. Blundell and P. J. Baker, *Nat. Chem.*, 2010, **2**, 1031–1036.
8 H. Liu, X. Shi, F. Xu, L. Zhang, W. Zhang, L. Chen, Q. Li, C. Uher, T. Day and G. J. Snyder, *Nat. Mater.*, 2012, **11**, 422–425.
9 Y. He, T. Day, T. Zhang, H. Liu, X. Shi, L. Chen and G. J. Snyder, *Adv. Mater.*, 2014, **26**, 3974–3978.
10 D. A. Keen, *J. Phys.: Condens. Matter*, 2002, **14**, R819.
11 A. K. Shukla, H. N. Vasan and C. N. R. Rao, *Proc. R. Soc. London, Ser. A*, 1981, **376**, 619.
12 T. A. Miller, J. S. Wittenberg, H. Wen, S. Connor, Y. Cui and A. M. Lindenberg, *Nat. Commun.*, 2013, **4**, 1369.
13 D. T. Schoen, C. Xie and Y. Cui, *J. Am. Chem. Soc.*, 2007, **129**, 4116–4117.
14 (*a*) S.-I. Ohkoshi, Y. Tsunobuchi, T. Matsuda, K. Hashimoto, A. Namai, F. Hakoe and H. Tokoro, *Nat. Chem.*, 2010, **2**, 539–545; (*b*) Q. Zhang, Y. Liu, X. Bu, T. Wu and P. Feng, *Angew. Chem., Int. Ed.*, 2008, **47**, 113–116; (*c*) W.-W. Xiong, J. Miao, K. Ye, Y. Wang, B. Liu and Q. Zhang, *Angew. Chem., Int. Ed.*, 2008, **54**, 546–550; (*d*) Y. Liu, Q. Lin, Q. Zhang, X. Bu and P. Feng, *Chem. – Eur. J.*, 2014, **20**, 8297–8301; (*e*) W.-W. Xiong,

J. Miao, P.-Z. Li, Y. Zhao, B. Liu and Q. Zhang, *CrystEngComm*, 2014, **16**, 5989–5992.
15 J. Liu, T. Gottschall, K. P. Skokov, J. D. Moore and O. G. Gutfleisch, *Nat. Mater.*, 2012, **11**, 620–626.
16 S. Ishiwata, Y. Shiomi, J. S. Lee, M. S. Bahramy, T. Suzuki, M. Uchida, R. Arita, Y. Taguchi and Y. Tokura, *Nat. Mater.*, 2013, **12**, 512–517.
17 S. N. Guin, J. Pan, A. Bhowmik, D. Sanyal, U. V. Waghmare and K. Biswas, *J. Am. Chem. Soc.*, 2014, **136**, 12712–12720.
18 (*a*) L.-D. Zhao, S.-H. Lo, Y. Zhang, H. Sun, G. Tan, C. Uher, C. Wolverton, V. P. Dravid and M. G. Kanatzidis, *Nature*, 2014, **508**, 373–377; (*b*) A. Banik, U. S. Shenoy, S. Anand, U. V. Waghmare and K. Biswas, *Chem. Mater.*, 2015, **27**, 581; (*c*) A. Banik and K. Biswas, *J. Mater. Chem. A*, 2014, **2**, 9620–9625; (*d*) A. Chatterjee, S. N. Guin and K. Biswas, *Phys. Chem. Chem. Phys.*, 2014, **16**, 14635–14639; (*e*) K. Biswas, J. He, Q. Zhang, G. Wang, C. Uher, V. P. Dravid and M. G. Kanatzidis, *Nat. Chem.*, 2011, **3**, 160–166; (*f*) Q. Zhang, C. D. Malliakas and M. G. Kanatzidis, *Inorg. Chem.*, 2009, **48**, 10910–10912.
19 L. Pan, D. Berardan and N. Dragoe, *J. Am. Chem. Soc.*, 2013, **135**, 4914–4917.
20 S. N. Guin and K. Biswas, *Chem. Mater.*, 2013, **25**, 3225–3231.
21 S. N. Guin, V. Srihari and K. Biswas, *J. Mater. Chem. A*, 2015, **3**, 648–655.
22 (*a*) S. N. Guin, A. Chatterjee, D. S. Negi, R. Datta and K. Biswas, *Energy Environ. Sci.*, 2013, **6**, 2603–2608; (*b*) S. N. Guin, A. Chatterjee and K. Biswas, *RSC Adv.*, 2014, **4**, 11811–11815.
23 O. Osters, M. Bawohl, J. L. Bobet, B. Chevalier, R. Decourt and T. Nilges, *Solid State Sci.*, 2011, **13**, 944–947.
24 T. Nilges, M. Bawohl, S. Lange, J. Messel and O. Osters, *J. Electron. Mater.*, 2010, **39**, 2096–2104.
25 S. Lange and T. Nilges, *Chem. Mater.*, 2006, **18**, 2538–2544.
26 T. Nilges, J. Messel, M. Bawohl and S. Lange, *Chem. Mater.*, 2008, **20**, 4080–4091.
27 T. Nilges and M. Bawohl, *Z. Naturforsch., B: J. Chem. Sci.*, 2008, **63**, 629–636.
28 R. Blachnik and G. Kudermann, *Z. Naturforsch., B: Anorg. Chem., Org. Chem.*, 1973, **28**, 1–4.
29 R. Blachnik and H. A. Dreisbach, *J. Solid State Chem.*, 1985, **60**, 115–122.
30 T. Doert, E. Rönsch, F. Schnieders, P. Böttcher and J. Sieler, *Z. Anorg. Allg. Chem.*, 2000, **626**, 89.
31 T. Nilges, S. Nilges, A. Pfitzner, T. Doert and P. Böttcher, *Chem. Mater.*, 2004, **16**, 806–812.
32 T. Nilges, C. Dreher and A. Hezinger, *Solid State Sci.*, 2005, **7**, 79–88.
33 T. Nilges and S. Lange, *Z. Anorg. Allg. Chem.*, 2005, **631**, 3002–3012.
34 M. Bawohl and T. Nilges, *Z. Naturforsch., B: J. Chem. Sci.*, 2008, **63**, 1083–1086.
35 J. Messel and T. Nilges, *Z. Naturforsch., B: J. Chem. Sci.*, 2008, **63**, 1077–1082.
36 T. Nilges, O. Osters, M. Bawohl, J.-L. Bobet, B. Chevalier, R. Decourt and R. Weihrich, *Chem. Mater.*, 2010, **22**, 2946–2954.
37 B. Reuter and K. Hardel, *Angew. Chem.*, 1960, **72**, 138–139.
38 T. Nilges and J. Messel, *Z. Anorg. Allg. Chem.*, 2008, **634**, 2185–2190.
39 S. Lange, M. Bawohl, D. Wilmer, H.-W. Meyer, H.-D. Wiemhöfer and T. Nilges, *Chem. Mater.*, 2007, **19**, 1401–1410.
40 T. Nilges, M. Bawohl and S. Lange, *Z. Naturforsch., B: J. Chem. Sci.*, 2007, **62**, 955–964.
41 S. Lange, M. Bawohl and T. Nilges, *Inorg. Chem.*, 2008, **47**, 2625–2633.
42 T. Nilges, M. Bawohl, J. Messel and O. Osters, *Z. Anorg. Allg. Chem.*, 2010, **636**, 15–18.
43 C. Xiao, Z. Li, K. Li, P. Huang and Y. Xie, *Acc. Chem. Res.*, 2014, **47**(4), 1287–1295.
44 H. Liu, X. Yuan, P. Lu, X. Shi, F. Xu, Y. He, Y. Tang, S. Bai, W. Zhang, L. Chen, Y. Lin, L. Shi, H. Lin, X. Gao, X. Zhang, H. Chi and C. Uher, *Adv. Mater.*, 2013, **25**, 6607–6612.
45 M. Giller, M. Bawohl, A. P. Gerstle and T. Nilges, *Z. Anorg. Allg. Chem.*, 2013, **639**, 2379–2381.
46 M. Faraday, *Philos. Trans. R. Soc. London*, 1833, **123**, 507–522.
47 S. D. Perez, M. A. Garcia, M. D. Garcia, G. B. Domene, C. Mühle and M. Jansen, *Inorg. Chem.*, 2013, **52**, 355–361.
48 D. M. Trots, A. N. Skomorokhov, M. Knapp and H. Fuess, *J. Phys.: Condens. Matter*, 2007, **19**, 136204.
49 S. Djurle, *Acta Chem. Scand.*, 1958, **12**, 1427–1436.
50 A. J. Hong, L. Li, H. X. Zhu, X. H. Zhou, Q. Y. He, W. S. Liu, Z. B. Yan, J.-M. Liu and Z. F. Ren, *Solid State Ionics*, 2014, **261**, 21–25.
51 C. Han, Q. Sun, Z. Cheng, J. Wang, Z. Li, M. G. Lu and S. Dou, *J. Am. Chem. Soc.*, 2014, **136**, 17626–17633.
52 D. T. Morelli, V. Jovovic and J. P. Heremans, *Phys. Rev. Lett.*, 2008, **101**, 035901.
53 M. D. Nielsen, V. Ozolins and J. P. Heremans, *Energy Environ. Sci.*, 2013, **6**, 570–578.
54 S. Geller and J. H. Wernick, *Acta Crystallogr.*, 1959, **12**, 46–54.
55 S. N. Guin, D. S. Negi, R. Datta and K. Biswas, *J. Mater. Chem. A*, 2014, **2**, 4324–4331.